Novel Polymer Composites Based on a Mixture of Preformed Nanosilica-Filled Poly(methyl methacrylate) Particles and a Diepoxy/Diamine Thermoset System

P. D. Castrillo, D. Olmos, J. González-Benito

Departamento de Ciencia e Ingeniería de Materiales e Ingeniería Química, Universidad Carlos III de Madrid, Avenida Universidad 30, 28911 Leganés, Madrid, Spain

Received 9 October 2007; accepted 17 June 2008
DOI 10.1002/app.29212
Published online 10 November 2008 in Wiley InterScience (www.interscience.wiley.com).

ABSTRACT: In this work, a new material based on an epoxy thermoset modified with a thermoplastic filled with silica nanoparticles was investigated. When thermoplastic particles are filled with nanoparticles with unique properties such as high efficiency for absorbing ultraviolet light, electric or magnetic shielding, high electrical conductivity, and high dielectric constants, more than an enhancement of the mechanical properties is expected to be achieved for modified epoxy-based thermosets. Particles of poly(methyl methacrylate) (PMMA) filled with silica nanoparticles were used to modify a thermoset based on a full reaction between diglycidyl ether of bisphenol A and 3-(aminomethyl)benzylamine. When the preformed thermoplastic particles were mixed with the reactive constituents of the epoxy system under certain curing conditions in which total miscibility was avoided, uniform particle dispersions could be obtained. The relationships between the composition, morphology (nanoscale and microscale), glass-transition temperature, mechanical properties, and fracture toughness were considered. Four main results were obtained for consideration of the potential of silica-filled PMMA as an important modifier of brittle epoxy thermoset systems: (1) a good dispersion of the silica nanoparticles in the PMMA domains, (2) a good dispersion of the silica-filled PMMA microparticles in the epoxy matrix, (3) the possibility of partial dissolution of the PMMA-rich domains into the epoxy system, and (4) a slight increase in properties such as the hardness, indentation modulus, and fracture toughness. © 2008 Wiley Periodicals, Inc. J Appl Polym Sci 111: 2062–2070, 2009

Key words: atomic force microscopy (AFM); hardness; interfaces; nanocomposites

INTRODUCTION

Blending polymers is an easy way of covering a large range of properties due to simply synergistic effects. In particular, modified epoxy systems have attracted special interest because an important requirement for certain applications is increasing their toughness and resistance to crack propagation. Among the possibilities for achieving those mechanical requirements, the addition of thermoplastics with high or relatively high glass-transition temperature (T_g) values[1–4] and the filling of epoxy thermosets with high-modulus materials (particles and fibers)[5] are perhaps the most used.

In the case of using particles as reinforcements, those fillers with dimensions on the nanoscale are very interesting because (1) the reduction of the particle size should inhibit crack propagation and (2) if good dispersion is achieved when the particle size is lower than the wavelength of visible light (as is the case with nanoparticles), transparent materials should be obtained.

On the other hand, the morphology is a significant factor influencing the properties of modified epoxy mixtures.[1,6–10] However, to reach a specific morphology when a thermoplastic is initially dissolved in one of the reactive components of the epoxy system is not an easy task because it depends on multiple factors: (1) the nature of the reactive components in the epoxy system, (2) the nature of the modifier, (3) the composition of the blend, and (4) the cure conditions. Many times, for these modified epoxy systems, morphologies in which the modifier-rich domains are immersed in the crosslinked epoxy polymer are preferred (e.g., to improve solvent resistance), but because of phase inversion, this issue is really difficult. In general, substantial amounts of the modifier are required to considerably improve the mechanical performance of the material; however, higher amounts of the modifier lead to phase inversion, in which the thermoplastic acts as the matrix.

Correspondence to: J. González-Benito (javid@ing.uc3m.es).

Contract grant sponsor: Project MAT2007-61607.

Probably, as reported Hayes and Seferis in a review,[11] the only way to get a specific morphology is to insert the domains of the modifier directly into the epoxy system before curing. In fact, there are a great number of papers and patents that focus their attention on the development of epoxy thermosets modified with preformed polymeric particles, demonstrating in many cases a clear toughness improvement.[11] However, most of them are related to preformed polymeric particles with low or relatively low T_g values; this induces a reduction of other properties such as stiffness in modified epoxy thermosets. Therefore, it is necessary to extend our knowledge about the effects of using preformed particles of thermoplastic polymers with high or relatively high T_g values and a relatively reduced size on the properties of the final material. In these systems, because of the similar densities of the polymeric constituents, it is reasonable to think that if the preformed thermoplastic particles are mixed with the reactive constituents of the epoxy system under certain curing conditions in which total miscibility is avoided, a uniform particle dispersion can be ensured, and so an effective transfer of their properties may be achieved. Furthermore, if the thermoplastic particles are filled with nanoparticles with unique properties such as high efficiency for absorbing ultraviolet light, electric or magnetic shielding, high electrical conductivity, and high dielectric constants, more than an enhancement of the mechanical properties might be attained.

In this work, a new material based on an epoxy thermoset modified with a thermoplastic filled with silica nanoparticles was studied. Particles of poly (methyl methacrylate) (PMMA) filled with silica nanoparticles were used to modify a thermoset based on the reaction between diglycidyl ether of bisphenol A (DGEBA) and 3-(aminomethyl)benzylamine (AMBA). The relationships between the composition, morphology (on the nanoscale and microscale), T_g, mechanical properties, and fracture toughness are considered.

EXPERIMENTAL

Materials

End-capped poly(bisphenol A-*co*-epichlorohydrin) glycidyl (i.e., DGEBA, Milwaukee, WI) with a number-average molecular weight of 348 g/mol (n = 0.03, where n represents an average contribution due to the presence of different oligomers) and 3-(aminomethyl)benzylamine (AMBA, II) were purchased from Aldrich Co.:

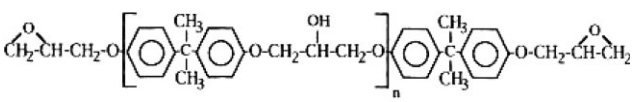

I

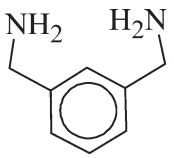

II

Fumed silica (SiO_2) nanoparticles with a 14-nm diameter were also purchased from Aldrich. PMMA (number-average molecular weight = 50,200, polydispersity = 1.5) was supplied by Atoglas S.A (Milan, Italy).

Sample preparation

First, microparticles of PMMA filled with silica nanoparticles were prepared as described elsewhere[12] by a high-energy blending process. PMMA and silica nanoparticles were mixed for 10 h with a proportion of 10 wt % silica particles. After that, the final composites were prepared in three steps: (1) mixtures of silica-filled PMMA (silica–PMMA) and DGEBA with different compositions (0, 1, 2, 3, 4, and 5 wt % in silica–PMMA) were prepared at room temperature, with the addition of silica–PMMA to DGEBA and vigorous stirring; (2) the hardener AMBA was poured in a stoichiometric amount with respect to the epoxy equivalents into every silica–PMMA/DGEBA mixture, which was prepared by vigorous stirring of the systems with a spatula for less than 2 min and pouring into a stainless steel mold with four parallelepipedic compartments (1 $\times$ 1 $\times$ 6 cm^3); and (3) finally, the blends were cured at 50°C for 4 h and postcured at 150°C for 2 h. Therefore, fully cured parallelepipedic specimens were prepared with dimensions of 1 $\times$ 1 $\times$ 6 cm^3 to be used in the fracture toughness tests. These tests were performed according to ASTM Standard Test Method D 5045-99 for the plane-strain fracture toughness (K_{Ic}) of plastic materials, for which only three specimens were required. In principle, with the same stainless steel mold in the same oven under the same conditions, it is more than reasonable to assume that the properties of the specimens will be the same within the error given by the data obtained from only one set of samples.

On the other hand, circular plates of the silica–PMMA nanocomposite (diameter = 20 mm and thickness = 1.5 mm) were prepared by injection molding with a Haake MiniJet (injection pressure = 550 bar at 6 s, postinjection pressure = 350 bar at 8 s, mold temperature = 80°C, and cylinder temperature = 210°C) (Karlsruhe, Germany).

Analytical techniques

Atomic force microscopy (AFM)

AFM studies were performed with a MultiMode Nanoscope IVA scanning probe microscope (Digital

Instruments/Veeco Metrology Group). All measurements were carried out under ambient conditions in the tapping mode with etched silicon probes (stiffness = 40 N/m). The driving frequency of the probe was adjusted to the resonant frequency in the immediate vicinity of the samples. Only topographical images were considered. In particular, to obtain high-resolution images, very light tapping was necessary. However, under those scanning conditions, phase contrast images did not clearly evidence differences between organic and inorganic phases. To overcome the latter, harder tapping was proven, but in this case, the spatial resolution was not sufficient to clearly show the nanoparticles.

Scanning electron microscopy (SEM)

The freeze-fractured surfaces of the fully cured silica–PMMA/epoxy specimens were imaged with a Philips XL30 scanning electron microscope, whereas the microanalysis at specific sites of the surfaces was performed with a DX4i coupled energy-dispersive X-ray spectroscopy (EDAX) detector. To avoid charge accumulation on the surfaces to be analyzed, the samples were coated with Au with the sputtering method. Backscattered electrons (BSEs) were used to simply examine the topography and to image the silica distribution over the freeze-fractured surfaces.

Differential scanning calorimetry

The calorimetric measurements were performed with a PerkinElmer Diamond differential scanning calorimeter (Waltham, MA). Pure indium was used as a standard for calorimetric calibration. Scans were carried out with an empty aluminum cell as the reference. The T_g values for the fully cured samples were determined from the inflexion point of the DSC traces obtained dynamically from 40 to 180°C at 10°C/min in a nitrogen atmosphere. The second heating scan of the cycle [40–180 (10°C/min), 180–40 (100°C/min), and 40–180°C (10°C/min)] was selected for the T_g determination to ensure the same thermal history for all the samples studied.

Microhardness

Martens microhardness measurements were performed with a Zwick/Roell machine (Ulm, Germany) with the following machine data: 2.5S1S WN:159229, crosshead travel monitor WN:159229, force sensor ID:0 WN:159230 2.5 kN, and universal hardness (HU) measurement head ID:25 WN:159231. The testing method was the Martens hardness method with a point of load application of 5 N, a speed load application of 1 mm/min, and a speed load removal of 1 mm/min. For every sample, at least 10 microhardness measurements were carried out along the long axis of the prepared specimens, the final data being given as the average.

Fracture toughness test

Toughness characterization of the prepared composites was performed according to ASTM Standard Test Method D 5045-99 for PMMA of plastic materials with a Shimadzu Autograph AG-I universal testing machine (Barcelona, Spain) equipped with a 1 kN load cell. Tests were carried out at room temperature (21°C) with a crosshead rate of 10 mm · min^{-1}. The critical stress intensity factor or K_{Ic} and the experimental fracture energy [or critical strain energy release rate (G_{Ic})] were obtained from three-point-bending tests performed on single-edge-notched fully cured specimens. The specimens to be tested were notched by machining and precracked with a natural crack initiated by the insertion and sliding of a new razor blade. The length of the overall crack was measured after the fracture experiment by observation with an optical microscope equipped with a video camera.

K_{Ic} was calculated as follows:

$$K_{Ic} = \left(\frac{P_{\max}}{BW^{1/2}}\right) \times f(x) \tag{1}$$

where P_{max}, B, W, and a are the maximum load in the fracture test, specimen thickness, specimen width, and crack length as determined with ASTM Standard D 5045-99, respectively. $f(x) = f(a/W)$ is a geometry factor given by

$$f(x) = 6x^{1/2}\frac{\left[1.99 - x(1-x)\left(2.15 - 3.93x + 2.7x^2\right)\right]}{(1+2x)(1-x)^{3/2}} \tag{2}$$

G_{Ic} was estimated with the following equation:

$$G_{Ic} = \frac{\left(1-\nu^2\right)\cdot K_{Ic}^2}{E} \tag{3}$$

where ν is Poisson's ratio (taken to be 0.35) and E is the modulus obtained with a three-point-bending test with the same rate test used for the fracture tests [instead of E, in this work, as an approximation and only with the intention of future comparisons between the materials under study, the values of the indentation modulus (Y_{HU}) obtained from the microhardness tests were taken].

RESULTS AND DISCUSSION

In Figure 1, as an example, two AFM height images of a freeze-fractured surface of a silica–PMMA/epoxy sample with 5 wt % silica–PMMA are shown.

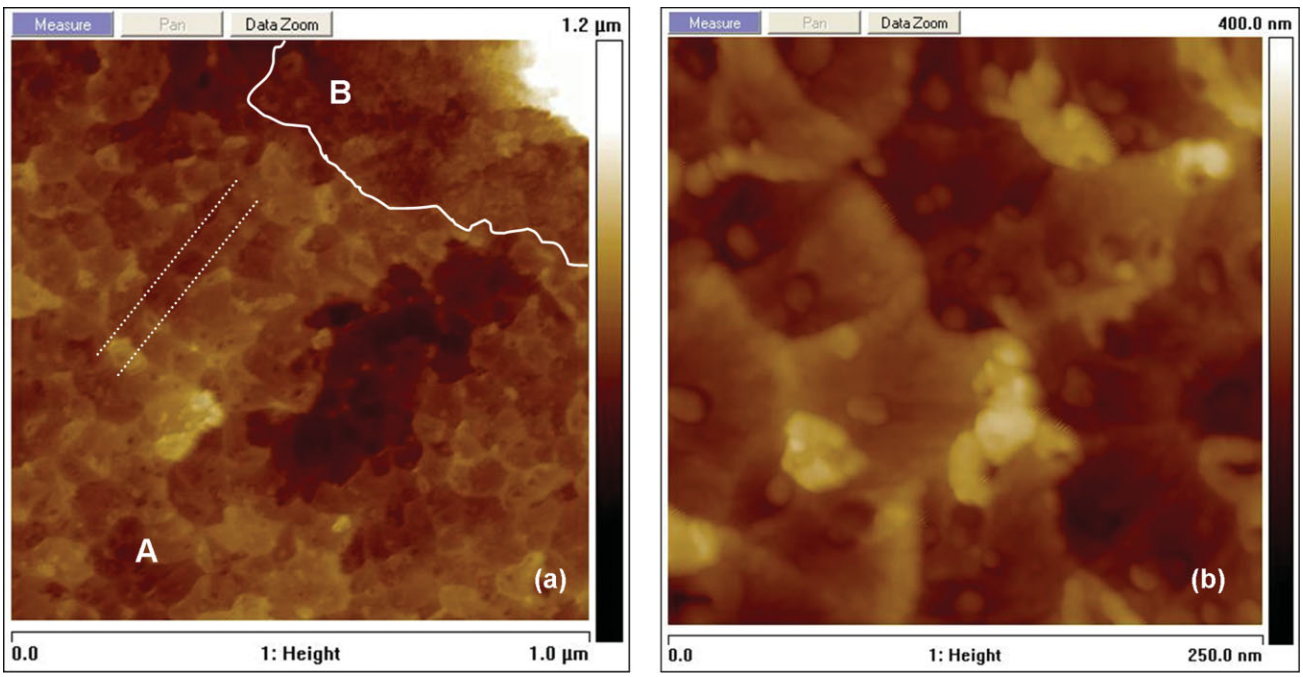

Figure 1 Tapping-mode AFM height images for the modified epoxy system with 5 wt % silica–PMMA particles. The scan sizes were 1 µm (left) and 250 nm (right). [Color figure can be viewed in the online issue, which is available at www.interscience.wiley.com.]

Two different regions can be seen on the top image of Figure 1: (1) region A with flake-shaped holes that seem to be arranged in a particular direction (dotted lines) and (2) region B with a more uniform granulated topography. Moreover, in region A, although not very clear, small balls and holes in the range of 10–20 nm can be observed. The last observation was confirmed by the scanning of an image with a higher resolution (right image of Fig. 1). In the right image of Figure 1, small balls with diameters close to 14 nm can be observed, indicating the presence of silica nanoparticles. Besides, it is interesting to highlight the very uniform distribution of the silica nanoparticles in the PMMA-rich domains, which, when we consider the relatively high proportion of nanoparticles for this kind of system (10 wt %), is more than successful. This result has been confirmed elsewhere by the inspection of the surfaces of fractured samples of pure nanosilica-filled PMMA.[12] When we take into account that the particles are placed nearly in the center of holes with a diameter of about 60 nm (right of Fig. 1), they seem to cause the specific fracture giving the flakelike texture observed in Figure 1. On the other hand, because the silica particles are occluded in the PMMA particles, it is reasonable to think that region A corresponds to a PMMA-rich domain, whereas region B must correspond to the epoxy matrix region. In fact, the kind of fracture observed in region A is in accordance with a typical ductile fracture mechanism in which by the coalescence of microcavities or, in this case, nanocavities, a crack is propagated by shear strain in a preferential direction (see the dotted lines in the left image of Fig. 1) in which the shear strength is maximum. This result suggests, therefore, that the added preformed silica–PMMA particles act as toughness modifiers, absorbing part of the applied load to plastically deform the PMMA-rich domains.

Additionally, Figure 2 shows a magnification of the right image of Figure 1 and a cross-section profile of one of the typical particles. The diameter of the particles was measured very accurately; a value of 14.2 nm was found that perfectly coincides with the diameter specified for the commercial silica particles used in this work.

In Figure 3(a), a typical image from BSEs of the silica–PMMA/epoxy (5 wt % silica–PMMA) sample is shown. In addition to certain topographical peculiarities mainly due to the kind of fracture, a black and white contrast can be observed, revealing few domains without any specific shape uniformly distributed in the region of observation that must reflect regions with different elemental compositions (this observation was made in different areas of the same sample and other samples). To determine the specific composition of those domains with respect to the rest of the sample, EDAX microanalysis was carried out. In Figure 3(b), typical X-ray dispersion energy spectra of the two kinds of regions on the analyzed surfaces are shown. The lighter regions clearly have silicon in their composition, whereas

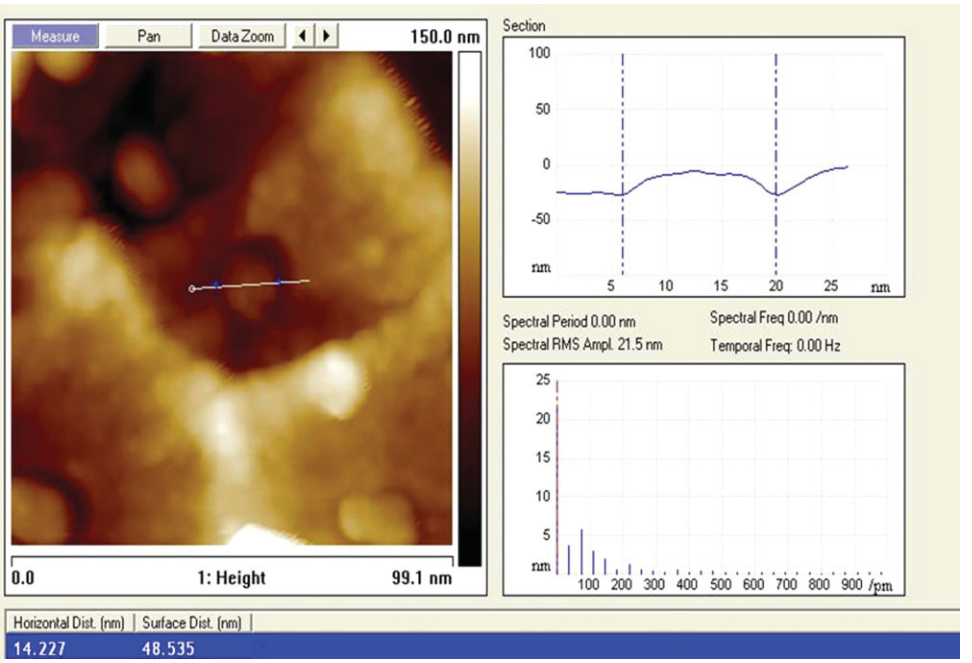

Figure 2 Zoom (left) and cross-section profiles (right) showing the actual size of one silica nanoparticle. [Color figure can be viewed in the online issue, which is available at www.interscience.wiley.com.]

the darker regions do not. These results suggest that the lighter regions correspond to the silica-filled PMMA domains.

In Figure 4, another BSE image of the epoxy/silica-filled PMMA (5 wt % silica-filled PMMA) sample is shown. In this case, although it is not as clear as the AFM images, the different surface texture observed for the silica-filled PMMA domains (arrow in Fig. 4), confirmed by EDAX analysis, points to a different kind of fracture mechanism in these regions with respect to that of the epoxy-rich phase, which points out again that the nanosilica-filled PMMA domains are actually acting as real toughness modifiers. With BSE, there are no clearly identifiable toughening mechanisms, perhaps because of the complexity of the system and lower spatial resolution in comparison with AFM; however, looking at the image of Figure 4, we find that when the crack reaches the PMMA-rich domain, the presence of the silica nanoparticles induces the creation of multiple microcavities and nanocavities, which subsequently generate the microcracks and nanocracks that must be the cause of the different texture observed in the PMMA-rich domain. However, as presented later, the microhardness and fracture tests are the experiments that should confirm the simple fractographic analysis performed with the visual inspection of AFM and BSE images.

Variations in the molecular dynamics of the composites can be studied with conventional DSC

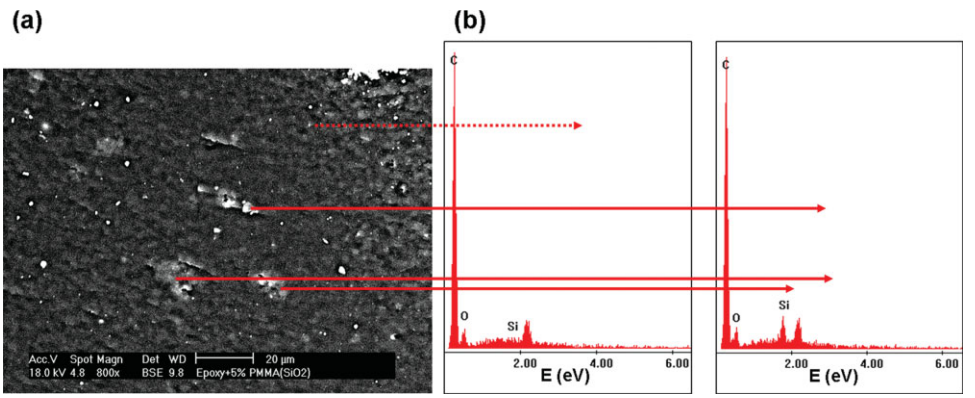

Figure 3 (a) BSE image of the modified epoxy system with 5 wt % silica–PMMA particles and (b) EDAX analysis of the polymer bulk (left) and some silica–PMMA domains (right). The peaks without a label at about 2 eV correspond to the signal coming from the presence of the Au coating. [Color figure can be viewed in the online issue, which is available at www.interscience.wiley.com.]

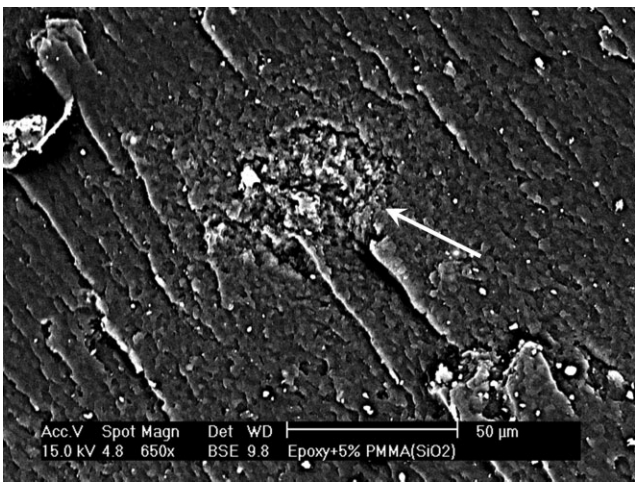

Figure 4 BSE image showing a detail of the silica–PMMA-rich domains.

experiments. For the samples under study, only one change was observed in the specific heat along the DSC trace, indicating the possibility of obtaining only one T_g. Taking into account the heterogeneity observed by either AFM and SEM, one would expect to obtain two T_g values, one corresponding to the epoxy matrix and the other to the nanosilica-filled PMMA-rich domains. Because the amount of the sample used to obtain the thermograms was about 10 mg, even for the sample with 5 wt % silica–PMMA, the amount of PMMA was so low that the equipment was not expected to be sufficiently sensitive to detect the glass transition associated with the thermoplastic. However, the T_g values of all the prepared samples (Table I) seemed to decrease very slightly as a function of the silica–PMMA content within the range of compositions under study. This slight decrease was about 3°C from 0 to 5 wt % silica–PMMA.

If total miscibility between the PMMA and the epoxy matrix were assumed during the short period of time from the initial mixture of silica–PMMA with DGEBA to the gel point of the epoxy–amine reactive components, one would expect only one T_g corresponding to the polymer solution. The estimation of T_g for ideal polymer blends using the Fox equation [eq. (4)] should give a reduction of about 4°C in the T_g value of the composite with 5 wt % silica–PMMA:

$$\frac{1}{T_g} = \frac{W_1}{T_{g1}} + \frac{W_2}{T_{g2}} \tag{4}$$

where T_g, T_{g1}, and T_{g2} are the glass-transition temperatures of the blend, the epoxy (132°C), and the silica–PMMA (85°C), respectively, and W_1 and W_2 are the weight fractions of the epoxy and silica–PMMA, respectively. This estimation, which differs by only 1°C from the T_g value obtained experimentally, suggests, therefore, that an important part of PMMA must have been dissolved by the epoxy reactive mixture. However, one must be very careful when considering these results, taking into account the small variations in T_g observed and the accuracy of the equipment.

On the other hand, to study the mechanical properties of the prepared composites, at least 10 indentations were made along the long axis of the specimens. This indentation procedure allowed us to reach a double objective: on the one hand to have an idea of the heterogeneity of the samples from a mechanical point of view and on the other hand to have an average of several mechanical properties.

In Figure 5, as an example, the indentation curves of the 2 wt % silica–PMMA specimen are presented. The rest of the samples showed similar curves.

From these curves, two mechanical parameters were obtained, and they are collected in Table I (HU and Y_{HU}).

HU is defined as the test force divided by the apparent area of the indentation under the applied test force. On the other hand, Y_{HU} can be calculated from the slope of the tangent of the indentation depth curve (as those in Fig. 5) at the maximum force with the indentation depth axis in millimeters and is comparable to the modulus of elasticity of the material (DIN Standard 50359-1).

TABLE I
T_g, HU, Y_{HU}, K_{Ic}, and G_{Ic} Values for the Different Composites

Composition (% silica–PMMA)	T_g (°C)	HU (N/mm^2)	Y_{HU} (kN/mm^2)	K_{Ic} (MPa · m$^{1/2}$)	G_{Ic} (kJ/m^2)
0	132.2	143 ± 2	3.80 ± 0.07	1.41 ± 0.28	0.47
1	134.2	136 ± 3	3.74 ± 0.05	1.22 ± 0.13	0.35
2	130.3	138 ± 4	3.75 ± 0.10	1.45 ± 0.22	0.49
3	129.8	147 ± 9	3.96 ± 0.21	1.44 ± 0.28	0.48
4	130.5	146 ± 3	3.96 ± 0.07	1.60 ± 0.33	0.57
5	129.3	146 ± 2	3.96 ± 0.04	1.34 ± 0.28	0.42
100	85[a]	158 ± 24	4.95 ± 0.68	—	

[a] The data were obtained from ref. 12.

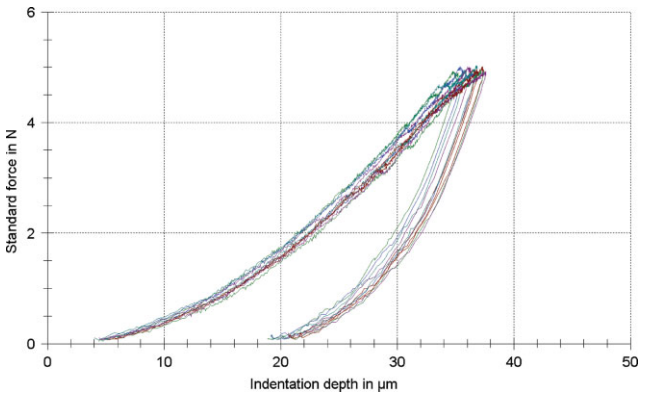

Figure 5 Indentation curves of the 2 wt % silica–PMMA specimen. [Color figure can be viewed in the online issue, which is available at www.interscience.wiley.com.]

Despite at least 10 indentations along the long axis of the specimen, after the first analysis, a few measurements were rejected because their data were very far away from the rest. This result was considered due to the possible presence of microdefects at the surface of the specimens, which might have affected the measurements. Therefore, the points considered for the statistical analysis were always in a reasonable confidence interval, with at least 7 points used in every case for the analysis. Besides, as an example, in Figure 6, HU and Y_{HU} are represented as functions of the distance along the long axis of one specimen of the sample with 5 wt % silica–PMMA. The consistency of these results suggests a good distribution of the silica–PMMA component within the epoxy matrix. As proof, the lines corresponding to average values of HU and Y_{HU} for the samples with 0 and 100% silica–PMMA are shown in Figure 6.

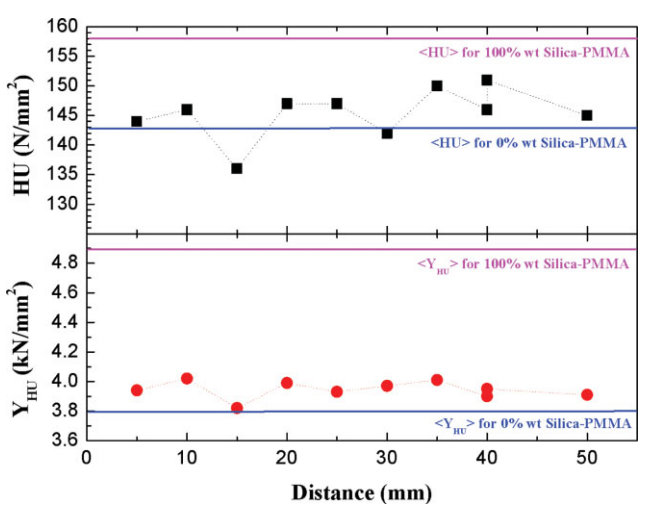

Figure 6 HU and Y_{HU} as a function of the distance along the long axis of one specimen of a sample with 5 wt % silica–PMMA. [Color figure can be viewed in the online issue, which is available at www.interscience.wiley.com.]

On the other hand, Table I shows that within the experimental error there is almost no variation in HU and Y_{HU} when the amount of the nanosilica-filled thermoplastic increases. However, in Figure 7, the values of the obtained mechanical parameters, HU and Y_{HU}, as a function of the composite composition are represented for a better visualization of the tendencies. Without consideration of the errors, there exist two regions: the first one extends to the case in which 1 wt % silica–PMMA is added and both parameters decrease, and the second region starts from 2 wt % silica–PMMA, for which HU and Y_{HU} seem to increase until reaching the values for the pure silica–PMMA material.

The increase in the values of HU and Y_{HU} with the addition of 2 wt % silica–PMMA might be explained by good adherence between the two components; in fact, although relatively close, the mixture rule ($Y_{HU} = \phi_1 Y_{HU}^{(1)} + \phi_2 Y_{HU}^{(2)}$, where Y_{HU} and $Y_{HU}^{(i)}$ are the indentation moduli of the composite and component i, respectively, and ϕ_i is the volume fraction of component i) underestimates these parameters (Fig. 7). A possible explanation of this behavior might be given by the partial dissolution of

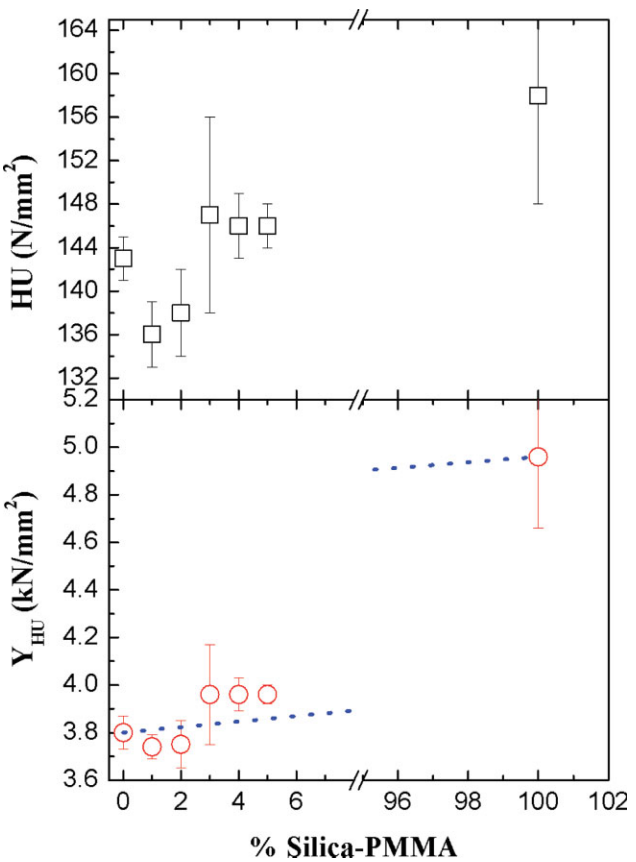

Figure 7 HU and Y_{HU} as a function of the composite composition. The dotted line represents the mixture rule. [Color figure can be viewed in the online issue, which is available at www.interscience.wiley.com.]

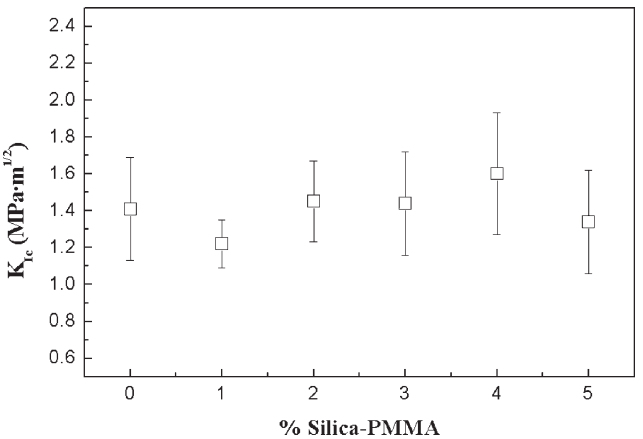

Figure 8 K_{Ic} as a function of the composite composition.

the PMMA-rich particles into the epoxy component, which would allow a favorable transmission of load, avoiding interfacial failures. This possibility is really interesting because one would expect the presence of an interphase with a gradient in mechanical properties between the PMMA domains and the epoxy matrix. In other words, this interphase would gradually absorb the mechanical energy, avoiding fast crack propagation as the BSE image in Figure 4 indicates. Figure 4 shows how the crack propagation is stopped when it reaches the PMMA-rich domain.

Finally, the influence of adding nanosilica-filled PMMA to the epoxy thermoset on the resistance of the material to fracture was investigated with fracture toughness tests. The values of K_{Ic} and G_{Ic} with different amounts of silica–PMMA in the composites are collected in Table I. K_{Ic} is a toughness parameter indicative of the resistance of a material to fracture, whereas G_{Ic} is a toughness parameter based on the energy required to fracture. As can be observed by taking into account the errors, at least in the range of compositions considered, we found no variation of toughness. However, if a representation of the data is made according to Figure 8, a tendency in the fracture toughness can be observed that is similar to the case of HU and Y_{HU} (the same happens for G_{Ic}), and this suggests that these properties are interconnected. A similar trend in the values of G_{Ic} can be observed in a recent work,[13] which shows a slight decrease in the value of G_{Ic} when the amount of silica nanoparticles increases from approximately 5 to 7% (v/v), although the observed differences are relatively small and probably within the experimental error. Also, Xu and Van Hoa[14] studied epoxy–clay nanocomposite systems as a function of the clay loading. In that work, a decrease was observed in the flexural resistance of the materials when the loading was over 4 phr. Nevertheless, it should also be taken into account that the materials under study are multicomponent systems, so a higher dispersion of the values of the mechanical properties can be expected. In particular, in this work, we are dealing with microcomposites (because of the size of the PMMA-filled particles) and nanocomposites (because of the size of the silica nanoparticles), and this broadens the spectra of possible interactions in this kind of system, its nature therefore being more complicated than that of a mere particle-filled composite. On the whole, the tendencies observed here point out that the mechanical resistance, stiffness, and fracture toughness of the selected model epoxy thermoset are improved when preformed particles of nanosilica-filled PMMA are added to the epoxy polymer.

In general, when a thermoplastic is used to modify an epoxy-based thermoset, the fracture toughness is significantly improved only when bicontinuous or inverted structures are generated, resulting from the plastic drawing of the thermoplastic-rich phase.[7,15–17] For the system under study, as preformed thermoplastic particles are added to the epoxy reactive mixture, avoiding phase inversion only an improvement of the toughness can be justified by the good interfacial adhesion due to the partial dissolution previously mentioned.

CONCLUSIONS

In this work, preformed particles of PMMA filled with silica nanoparticles (silica–PMMA) were used to modify a thermosetting epoxy polymer. SEM together with EDAX microanalysis revealed the existence of silica–PMMA domains uniformly distributed throughout the sample, whereas AFM allowed us to confirm the presence of 14-nm silica nanoparticles in PMMA-rich domains.

It is clear, therefore, that the results indicate that it is possible to obtain very easily a new sort of multicomponent system (ternary epoxy-based nanocomposites) in which an epoxy-based thermoset is modified with a silica-filled thermoplastic (PMMA). Four main results have been obtained for considering the potential of silica-filled PMMA as an important toughness modifier of brittle thermoset epoxy systems: (1) a good distribution of the silica nanoparticles in the PMMA domains, (2) an excellent distribution of the silica-filled PMMA microparticles in the epoxy matrix, (3) partial dissolution of the PMMA-rich domains (at the edges of the silica–PMMA particles) into the epoxy system, and (4) an increase in properties such as the hardness, Y_{HU}, and fracture toughness. Actually, maintaining or even increasing the mechanical properties, these new materials offer the possibility of introducing other kinds of properties from the incorporation of inorganic nanoparticles with unique properties.

The authors appreciate the help that they received from the Structures and Continuous Media Department of

Universidad Carlos III Madrid in making the notches in the specimens for the fracture tests, and they particularly appreciate the advice that they received from José Fernández Saez for performing the fracture tests. Finally, they thank the Materials and Technology group of Universidad del País Vasco for preparing by injection molding the discs of silica–PMMA composites.

References

1. Pascault, J. P.; Verdu, J.; Williams, R. J. J. Thermosetting Polymers; Marcel Dekker: New York, 2002.
2. Hedrick, J. L.; Yilgör, I.; Wilkes, G. L.; McGrath, J. E. Polym Bull 1985, 13, 201.
3. Pearson, R. A. In Toughened Plastics I: Science and Engineering; Riew, C. K.; Kinloch, A. J., Eds.; Advances in Chemistry Series 233; American Chemical Society: Washington, DC, 1993; p 405.
4. Hodgkin, J. H.; Simon, G. P.; Varley. R. J. Polym Adv Technol 1998, 9, 3.
5. Jang, B. Z. Advanced Polymer Composites; ASM International: Materials Park, OH, 1994.
6. Williams, R. J. J.; Rozenberg, B. A.; Pascault, J. P. Adv Polym Sci 1997, 128, 95.
7. Girard-Reydet, E.; Vicard, V.; Pascault, J. P.; Sautereau, H. J Appl Polym Sci 1997, 65, 2433.
8. Verchére, D.; Pascault, J. P.; Sautereau, H.; Moschiar, S. M.; Riccardi, C. C.; Williams, R. J. J. J Appl Polym Sci 1991, 43, 293.
9. Kinloch, A. J.; Yuen, M. L.; Jenkins, S. D. J Mater Sci 1994, 29, 3781.
10. Schauer, E.; Berglund, L.; Pena, G.; Marieta, C.; Mondragón, I. Polymer 2002, 43, 1241.
11. Hayes, B. S.; Seferis, J. C. Polym Compos 2001, 22, 451.
12. Castrillo, P. D.; Olmos, D.; Amador, D. R.; González-Benito, J. J Colloid Interface Sci 2007, 308, 318.
13. Johnsen, B. B.; Kinloch, A. J.; Mohammed, R. D.; Taylor, A. C.; Sprenger, S. Polymer 2007, 48, 530.
14. Xu, Y.; Van Hoa, S. Compos Sci Technol 2008, 68, 854.
15. MacKinnon, A. J.; Jenkins, S. D.; McGrail, P. T.; Pethrick, R. A. Macromolecules 1992, 25, 3492.
16. Kinloch, A. J.; Yuen, M. L.; Jenkins, S. D. J Mater Sci 1994, 29, 3781.
17. Venderbosch, R. W.; Meijer, H. E. H.; Lemstra, P. J. Polymer 1994, 35, 4349.